



# **Influence of EGR unequal distribution from cylinder to cylinder on NO<sub>x</sub>-PM trade-off of a HSDI automotive Diesel engine**

Alain Maiboom, Xavier Tauzia, Jean-François Hétet

## **► To cite this version:**

Alain Maiboom, Xavier Tauzia, Jean-François Hétet. Influence of EGR unequal distribution from cylinder to cylinder on NO<sub>x</sub>-PM trade-off of a HSDI automotive Diesel engine. *Applied Thermal Engineering*, 2009, 29 (10), pp.2043. <10.1016/j.applthermaleng.2008.10.017>. <hal-00505530>

**HAL Id: hal-00505530**

**<https://hal.science/hal-00505530v1>**

Submitted on 24 Jul 2010

**HAL** is a multi-disciplinary open access archive for the deposit and dissemination of scientific research documents, whether they are published or not. The documents may come from teaching and research institutions in France or abroad, or from public or private research centers.

L'archive ouverte pluridisciplinaire **HAL**, est destinée au dépôt et à la diffusion de documents scientifiques de niveau recherche, publiés ou non, émanant des établissements d'enseignement et de recherche français ou étrangers, des laboratoires publics ou privés.



HAL Authorization

## Accepted Manuscript

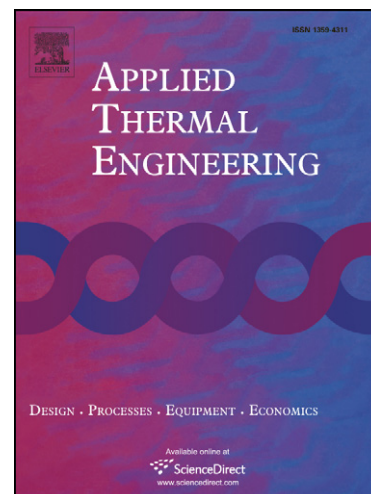
Influence of EGR unequal distribution from cylinder to cylinder on NO<sub>x</sub>-PM trade-off of a HSDI automotive Diesel engine

Alain Maiboom, Xavier Tauzia, Jean-François Hétet

PII: S1359-4311(08)00422-5  
DOI: [10.1016/j.applthermaleng.2008.10.017](https://doi.org/10.1016/j.applthermaleng.2008.10.017)  
Reference: ATE 2642

To appear in: *Applied Thermal Engineering*

Received Date: 26 May 2008  
Revised Date: 9 October 2008  
Accepted Date: 22 October 2008



Please cite this article as: A. Maiboom, X. Tauzia, J-F. Hétet, Influence of EGR unequal distribution from cylinder to cylinder on NO<sub>x</sub>-PM trade-off of a HSDI automotive Diesel engine, *Applied Thermal Engineering* (2008), doi: [10.1016/j.applthermaleng.2008.10.017](https://doi.org/10.1016/j.applthermaleng.2008.10.017)

This is a PDF file of an unedited manuscript that has been accepted for publication. As a service to our customers we are providing this early version of the manuscript. The manuscript will undergo copyediting, typesetting, and review of the resulting proof before it is published in its final form. Please note that during the production process errors may be discovered which could affect the content, and all legal disclaimers that apply to the journal pertain.

## Influence of EGR unequal distribution from cylinder to cylinder on NO<sub>x</sub>-PM trade-off of a HSDI automotive Diesel engine

Alain Maiboom<sup>\*</sup>, Xavier Tauzia, Jean-François Hétet

Internal Combustion Engine Team,  
Laboratory of Fluid Mechanics, UMR 6598 CNRS,  
Ecole Centrale de Nantes,  
BP 92101, 44321 Nantes Cedex 3, France

### Abstract

The influence of cylinder-to-cylinder variation in EGR distribution on the NO<sub>x</sub>-PM trade-off (while varying EGR rate) is studied on an automotive high-speed direct injection Diesel engine. Experiments have been conducted on an engine test bench with and without air-EGR mixer and demonstrate that variations in cylinder-to-cylinder EGR distribution results in a deteriorated NO<sub>x</sub>-PM trade-off (increased NO<sub>x</sub> emissions level at a given PM emissions level, or increased PM emissions level at a given NO<sub>x</sub> emissions level) compared to the well mixed configuration with equal EGR rate for all the cylinders. A qualitative study as well an original experiment is conducted to explain this emissions increase induced by unequal distribution of EGR. When recirculating hot exhaust gases, the emissions increase is due to cylinder-to-cylinder variations in intake gas composition and temperature.

Keywords: Diesel engine; pollutant emissions; exhaust gas recirculation (EGR); unequal cylinder-to-cylinder EGR distribution; EGR maldistribution; NO<sub>x</sub>-PM trade-off

<sup>\*</sup> Corresponding author

Tel: +33 2 40 37 68 80; Fax: +33 2 40 37 25 56

E-mail address: alain.maiboom@ec-nantes.fr

### Nomenclature

[CO <sub>2</sub> ]	CO <sub>2</sub> concentration (%)
D	volume flow (m <sup>3</sup> .s <sup>-1</sup> )
$\dot{m}$	mass flow (kg.s <sup>-1</sup> )
$\dot{n}$	molar flow (mol.s <sup>-1</sup> )
NO <sub>x</sub> (g/h)	NO <sub>x</sub> emissions (g.h <sup>-1</sup> )
P	pressure (bar)
PM (g/h)	PM emissions (g.h <sup>-1</sup> )
T	temperature (K)

$X_{egr}$  EGR ratio (%)

*Greek letters*

$\rho$  density ( $\text{kg.m}^{-3}$ )

*Subscripts*

a air  
cool engine coolant  
ex exhaust  
egr related to recirculated exhaust gases  
in inlet  
mix after mixing with recirculated exhaust gases

*Abbreviations*

BMEP brake mean effective pressure  
BSFC brake specific fuel consumption  
DI direct injection  
EGR exhaust gas recirculation  
EUDC extra urban driving cycle  
FSN filter smoke number  
HP high pressure  
HSDI high speed direct injection  
HTC high temperature combustion  
LTC low temperature combustion  
PM particulate matter  
ROHR rate of heat release  
UDC urban driving cycle  
VGT variable geometry turbine

## 1. Introduction

Future emissions regulations like EURO 6 in Europe force Diesel engine manufacturers to find ever more complex ways to reduce exhaust gas pollutant emissions, in particular NO<sub>x</sub> and particulate matter (PM) emissions. Exhaust gas recirculation (EGR) into the engine intake is an established technology to reduce NO<sub>x</sub> emissions [1, 2]. The decrease of NO<sub>x</sub> emissions with EGR is the result of complex and sometimes opposite phenomena occurring during combustion [3-10].

At the same time, the decrease in combustion temperatures and oxygen concentration while increasing EGR rate reduces both soot production in the spray core and soot oxidation in the diffusion flame around the jet [11]. Thus the final impact of EGR on PM emissions is complex and is the result of contradictory phenomena. In the conventional Diesel high-temperature combustion (HTC), the increase of EGR rate (at constant boost pressure) is accompanied by an increase of PM emissions, resulting in a trade-off between NO<sub>x</sub> and PM emissions while varying EGR rate [4, 12-15].

Moreover, practical EGR systems often lead to EGR unequal distribution from cylinder to cylinder, air and EGR being imperfectly mixed. This phenomenon has been studied by various researchers [16-24]. By measuring CO<sub>2</sub> instantaneous concentration at each inlet port during the intake stroke owing to mid-infrared laser absorption spectroscopy, Green [16] has demonstrated that even when operating at a steady condition, the engine's EGR system can produce large temporal variations in the EGR concentration within the flow of fresh charge during the intake stroke, that are different for each cylinder. Furthermore, CFD analyses [17-18, 20-21] have demonstrated that a standard engine's EGR system results in a highly stratified concentration field within the inlet manifold. Many experimental and numerical studies [17, 19, 23-24] have proposed improved inlet manifolds or air-EGR connections in order to improve cylinder-to-cylinder EGR distribution.

If some studies have shown that cylinder-to-cylinder variations in EGR can lead to higher NO<sub>x</sub> and PM emissions compared to a configuration where the EGR is equally distributed among all cylinders [17], the influence of on the NO<sub>x</sub>-PM trade-off (while varying EGR rate) has not been experimentally studied in details or explained. Thus, the aim of this study is to quantify and explain the influence of this phenomenon on the NO<sub>x</sub>-PM trade-off (while varying EGR rate at constant boost pressure) of an automotive HSDI Diesel engine.

## 2. Experimental setup

### 2.1. Test engine and operating conditions

Experiments are conducted on a 2.0 l constant-moderate-swirl, water-cooled, turbocharged inter-cooled HSDI Diesel engine, equipped with a variable geometry turbine (VGT) and a high pressure (HP) water-cooled EGR loop (recirculated gas are taken upstream of the turbine and introduced downstream of the compressor). Engine specifications are given in Table 1.

When opening EGR valve to increase EGR flow rate at a fixed VGT vanes position, boost pressure is reduced because of a reduced exhaust gas flow through the turbine. Boost pressure is maintained constant by closing VGT vanes when opening EGR valve. Thus, both EGR flow rate and boost pressure are controlled simultaneously.

An air-EGR mixer was developed to ensure that air and recirculated gases are perfectly mixed to suppress cylinder-to-cylinder variations in EGR quantity. EGR gases are introduced into the main inlet duct tangentially, thus creating a vortex (Figure 1). Moreover, when using the air-EGR mixer, the volume of inlet duct between air-EGR mixer and inlet manifold is increased in order to limit the temporal variations in the EGR concentration. The influence of EGR unequal distribution on NO<sub>x</sub>-PM trade-off is thus obtained by comparing engine-out NO<sub>x</sub> and PM emissions with and without the air-EGR mixer (Figure 2). Inlet air temperature  $T_a$  (after intercooler) is controlled separately.

The study is conducted at part load and low load conditions (operating points A and B respectively), such as those encountered in the European emissions test cycle for light-duty vehicles – composed of four urban driving cycles (UDC) and one extra urban driving cycle (EUDC). The corresponding engine speed, pilot and main injection quantities, brake mean effective pressure (BMEP) and rail pressure are given in Table 2. For each operating point,

injection quantities are held constant, and thus the BMEP is little changed for the various operating conditions (use of air-EGR mixer, variation of EGR rate).

## 2.2. Emissions measurement and intake gas analysis

NOx emissions are measured with an ECO PHYSICS CLD 700EL gas analyser, which uses the chemical luminescence detector (CLD) method. PM emissions at the exhaust are measured with an AVL 415S smoke meter. The conversion of NOx emissions from ppm to g/h and the calculation of PM emissions in g/h starting from the filter smoke number (FSN) are explained in a previous paper [3].

Inlet and exhaust CO<sub>2</sub> concentrations are measured with a SIEMENS ULTRAMAT 23 gas analyser, which uses the non-dispersive infrared measurement technique (NDIR).

Each gas analyser is calibrated every 4 hours of experiments with specific gas standards. If the necessary shift is under 0.3 %, then the experiments done since the previous calibration are validated.

The EGR rate of cylinder  $j$  is defined as follows:

$$X_{egr,j}(\%) = 100 \cdot \frac{[CO_2]_{in,j}}{[CO_2]_{ex}} \quad (1)$$

Where  $[CO_2]_{in,j}$  and  $[CO_2]_{ex}$  are measured CO<sub>2</sub> concentrations at inlet port of cylinder  $j$  and exhaust manifold respectively (Figure 2).

The mean EGR rate is given by:

$$X_{egr}(\%) = \frac{1}{4} \sum_{j=1}^4 X_{egr,j}(\%) \quad (2)$$

As explained in the introduction, a standard engine's EGR system results in a high inhomogeneous EGR concentration field within the inlet manifold (in particular in the cross section of each intake port) and produces temporal variations in the EGR concentration during the intake stroke because of the pulsating flow induced by inlet valve opening and closure. As a consequence, the mean temporal value  $[CO_2]_{in,j}$  obtained with the gas analyser without air-EGR mixer is not representative of the real CO<sub>2</sub> concentration in the cylinder  $j$  at inlet valve closure. Also, the temporal mean value of the temperature  $T_{in,j}$  given by the thermocouple introduced in the flow of inlet port  $j$  is not representative of mean temperature of inlet gases introduced in the cylinder during intake stroke. It depends on the implementation of the thermocouple in the cross section. As for instance, if it is implemented in a high EGR concentration area of the cross section, it will overestimate the mean temperature of inlet gases in the cross section because recirculated gases are hotter than fresh air.

However, the comparison of individual EGR rates  $X_{egr,j}$  and individual intake temperatures  $T_{in,j}$  as defined earlier gives an estimation of the unequal distribution of EGR gases.

Only when using the air-EGR mixer with a large volume upstream of the inlet manifold, the EGR concentration field (and consequently the temperature field) within the inlet manifold is almost constant and uniform. Measured CO<sub>2</sub> concentrations and intake temperatures are consequently representative of CO<sub>2</sub> concentration and temperature of the

gases introduced in the cylinders during the intake stroke. When air and EGR are well mixed, all EGR rates are then equal:

$$X_{egr}(\%) = 100 \cdot \frac{[CO_2]_{mix}}{[CO_2]_{ex}} = X_{egr,j}(\%) \quad (3)$$

### 2.3. Error analysis

Table 3 sums up the measurement technique, calibrated range, accuracy and relative error of various instruments involved in the experiments described in this study for main parameters. Errors in experiments can arise from instrument conditions, calibration, environment, observation, reading and test planning. The accuracy of the experiments has to be validated with an error analysis. That is performed here using the differential method of propagating errors based on Taylor' theorem [25]. It gives the maximum error  $u$  of a function  $f(x_1, x_2, \dots, x_n)$  as follows:

$$u(f(x_1, x_2, \dots, x_n)) = \sqrt{\sum (c_i \cdot u(x_i))^2} \quad (4)$$

As a result, the maximum relative errors for  $X_{egr,j}$ , NOx (g/h), PM (g/h) are 1.4 %, 1.5 %, end 2.3 % respectively.

### 3. Experimental results: NOx-PM trade-offs with and without air/EGR mixer

The influence of EGR maldistribution on NOx-PM trade-off is obtained for both operating points A and B by increasing EGR rate with and without air-EGR mixer. The results are given on Figure 3. The EGR rate is increasing from 22 % to 34 % without air-EGR mixer and from 18 % to 30 % with air-EGR mixer for operating point A. It is increased from 26 % to 38 % for operating point B.

Boost pressure is maintained at a fixed level by closing VGT vanes when opening EGR valve, at 1070 mbar and 1120 mbar for operating points A and B respectively.

Moreover, as engine coolant passes through the EGR cooler with a constant flow rate, EGR temperature  $T_{egr}$  is increasing when increasing recirculated exhaust gases flow, whereas inlet air temperature  $T_a$  is maintained at a fixed value. As a matter of fact, the temperature  $T_{mix}$  of inlet gases after mixing with EGR is increasing as well, thus reducing the inlet gas density and in-cylinder trapped mass ("thermal throttling").

Injection parameters (timing and quantity of pilot and principal injections) are maintained while varying EGR rate. The influence of EGR on the gross ROHR and in-cylinder pressure trace is given on Figure 4 a and Figure 4 b respectively, for operating point B (with air-EGR mixer). The corresponding trends of the mean core spray temperature  $T_{3/4}$  (that controls the PM production) and the diffusion flame temperature  $T_5$  (that controls both the NOx production and the soot oxidation at the jet periphery in the diffusion flame) are calculated by a 6-zone phenomenological combustion model (presented in a previous paper [26]) and presented on Figure 4 c and d.

As depicted by other researchers [3][5] and Figure 4 b, the combustion process is delayed when increasing EGR rate (ignition delay, premixed combustion, diffusion and late diffusion combustion). Thus, the whole combustion process is shifted further into the

expansion stroke, leading to lower cylinder pressure (see Figure 4 a), lower BMEP, and consequently higher brake specific fuel consumption (BSFC): 3.3 % increase is observed for operating point A when increasing EGR rate from 18 % to 30 %, and 20 % for operating point B when increasing EGR rate from 25 % to 38 % (with air-EGR mixer).

As traditionally observed [2-4, 6-7, 9, 12-15], the increase of EGR rate results in a decrease of NO<sub>x</sub> emissions, whether with or without air-EGR mixer: 75 % decrease is observed for operating point A when increasing EGR rate from 18 % to 30 %, and 74 % for operating point B when increasing EGR rate from 25 % to 38 % (with air-EGR mixer). This decrease in NO<sub>x</sub> emissions is traditionally attributed to the decrease in the diffusion flame temperature (as depicted on Figure 4 d). The result of an increase of EGR rate on PM emissions is more complex.

- PM emissions are increased by 8.80 times (from 1.24 g/h to 10.90 g/h) for operating point A when increasing EGR rate from 18 % to 30 %.
- For operating point B, PM emissions are first increased as for operating point A, and then decreased for high EGR rates (over 36 %). As depicted on Figure 4 c, the core spray temperature where PM are produced becomes too low for PM formation (minimal temperature needed for soot inception: 1400 K [11]), thus entering a low temperature combustion (LTC) mode with low NO<sub>x</sub> and PM emissions, as described by other researchers [27-29]. This LTC combustion mode is accompanied with a large increase of CO and HC emissions, of 151 % and 158 % respectively when increasing EGR rate from 25 % to 38 % (with air-EGR mixer).

As depicted on Figure 3, the comparison between NO<sub>x</sub>-PM trade-offs obtained with and without air-EGR mixer demonstrates that unequal distribution of EGR gases results in deteriorated NO<sub>x</sub> and PM emissions. For instance for operating point A, for higher EGR rates tested, a decrease of 20 % NO<sub>x</sub> is obtained at a given PM emissions level, and 32 % reduction in PM emissions is obtained at a given NO<sub>x</sub> emissions level while utilising the air-EGR mixer compared to standard configuration. Corresponding measured CO<sub>2</sub> concentrations for operating point A with and without air-EGR mixer are given on Figure 5. For operating point A, it is shown that cylinder 4 seems to admit much more recirculated gases than cylinder 1, independently of mean EGR rate ; at 22% mean EGR rate,  $[CO_2]_{in,4}$  is 76% higher than  $[CO_2]_{in,1}$ . Measured intake temperatures  $T_{in,j}$  (not given here) are in the same order than CO<sub>2</sub> concentrations: the maximal CO<sub>2</sub> is accompanied to the maximal intake temperature. At the other hand, the differences in CO<sub>2</sub> concentration at each inlet port are very low when using the air-EGR mixer, at the same order of the accuracy of the CO<sub>2</sub> gas analyser ( $\pm 0.1$  %), showing that the air-EGR mixer is very efficient.

The shift between NO<sub>x</sub>-PM trade-offs is particularly important at high EGR rates for operating point B while entering a low NO<sub>x</sub> – low PM combustion mode (Figure 3 (b)).

#### 4. Explanation of the influence of unequal EGR distribution on NO<sub>x</sub>-PM trade-off

To explain the influence of unequal EGR distribution on NO<sub>x</sub> and PM emissions, two cases are studied. First one (Figure 6) considers a constant EGR temperature  $T_{egr}$ , at the same level that air temperature  $T_a$ . Second one (Figure 7) considers constant engine coolant temperature  $T_{cool}$  and flow rate through the EGR cooler, as on a standard engine



configuration.  $T_{egr}$  is thus higher than  $T_a$  and increases with EGR rate (because of a higher gas flow through the EGR cooler). Qualitative NO<sub>x</sub>-PM trade-offs (while varying EGR rate at constant boost pressure in the conventional HTC mode) given on Figure 6 and Figure 7 are obtained from measurements presented in last section and studies from the literature [30-31].

#### 4.1. Case 1: $T_{egr} = T_a$

In this first case, the NO<sub>x</sub>-PM trade-off (while varying EGR rate at constant  $T_{egr} = T_a$ ) gives NO<sub>x</sub> and PM emissions of each cylinder (Figure 6 (a) and (b)). Without proper EGR mixing, all cylinders have same emissions (designated as “well mixed” on Figure 6). When running with unequal EGR distribution, for example with one cylinder with a higher EGR rate, and another with a lower EGR rate, mean emissions are always higher than with proper EGR mixing in the classical HTC mode. With a low mean EGR rate, the shift between dispersed and well mixed configurations is low (Figure 6 (a)) because the NO<sub>x</sub> – PM trade-off is quasi linear for low EGR rates. The shift increases when increasing EGR rate (Figure 6 (b)).

#### 4.1. Case 2: $T_{egr} > T_a$

NO<sub>x</sub>-PM trade-offs while varying EGR rate at constant  $T_{egr} = T_a$  and constant engine coolant temperature  $T_{cool}$  ( $T_{egr} > T_a$ ) are plotted on Figure 7. As demonstrated by other researchers [30-31], NO<sub>x</sub>-PM trade off is improved when reducing exhaust gas temperature (reduced NO<sub>x</sub> emissions at a given PM emissions level, or reduced PM emissions at a given NO<sub>x</sub> emissions level). When increasing EGR rate at constant coolant temperature, inlet temperature  $T_{mix}$  is increasing for two reasons:

- ✓ The recirculated exhaust gases have a higher temperature than fresh air. Thus, the inlet temperature  $T_{mix}$  after mixing with recirculated gases increases with EGR rate.
- ✓ As the engine coolant temperature and flow through the EGR cooler are kept constant, the increase of EGR flow results in an increased EGR temperature.

As a consequence, the NO<sub>x</sub>-PM trade-off is better at constant  $T_{egr}$  than at constant  $T_{cool}$  ( $T_{egr} > T_a$ ).

Furthermore, when running with unequal EGR distribution, the cylinder that has a higher EGR rate (cylinder 1) has a higher inlet temperature ( $T_{high}$ ) as well, whereas the cylinder with the lower EGR rate (cylinder 2) has a lower inlet temperature ( $T_{low}$ ). NO<sub>x</sub>-PM trades-offs while maintaining inlet temperature at  $T_{low}$  and  $T_{high}$  are also plotted on Figure 7, the one with the low temperature being better than the one with the high temperature. It must be noticed that NO<sub>x</sub> and PM emissions of cylinder 1 and 2 are not placed on the NO<sub>x</sub>-PM trade-off at constant  $T_{cool}$  obtained on a multi-cylinder engine. Actually, for the cylinder with the high EGR rate, EGR temperature is unchanged compared to the well mixed configuration, whereas it is higher with the same EGR rate on the whole engine (because of an increased EGR temperature as explained earlier). As a matter of fact, cylinder one has a lower inlet temperature  $T_{mix}$  and thus little lower NO<sub>x</sub> and PM emissions than the corresponding point on the NO<sub>x</sub>-PM trade-off at constant  $T_{cool}$ .

Inversely, cylinder 2 has a higher inlet temperature and higher emissions than its corresponding point on the NO<sub>x</sub>-PM trade-off.

As in case 1, the dispersed configuration results in increased NO<sub>x</sub> and PM emissions.

As an example, a quantitative experiment is conducted for operating point A. NO<sub>x</sub> and PM emissions for the well mixed and dispersed configurations are obtained as explained below. First measurement consists in measuring NO<sub>x</sub> and PM emissions of the engine with 21.9 % EGR with the air-EGR mixer (without unequal EGR distribution). Corresponding intake CO<sub>2</sub> concentrations are equal to 2.2 %. Intake temperature  $T_{\text{mix}}$  is equal to 44.8°C ( $T_a = 24.0^\circ\text{C}$ ,  $T_{\text{egr}} = 156.5^\circ\text{C}$ ).

Then, for the same mean EGR rate, to model an EGR dispersion, it is supposed that two of the cylinders have a lower CO<sub>2</sub> concentration (1.6 %) and two others a higher one (2.8 %). Corresponding intake temperatures are calculated as explained in the appendix. These two intake configurations (intake CO<sub>2</sub> concentration and temperature) are simulated on the whole engine (four cylinders) with the air-EGR mixer. Contrary to previous experiments, an independently controlled water circuit on the EGR cooler is used to control the temperature of the recirculated gases  $T_{\text{egr}}$ , thus permitting control over the temperature  $T_{\text{mix}}$ . It is supposed that individual cylinder-out emissions are the same when EGR is properly mixed, thus giving each cylinder-out emissions of the engine with the simulated unequal EGR distribution. Global engine emissions (sum of individual cylinder-out emissions) are then compared to those obtained with proper EGR mixing. The results are given in Table 4.

For the well mixed configuration, it can be noticed that the shift between measured and calculated temperature  $T_{\text{mix}}$  is very low, at the same order that the accuracy of the thermocouple ( $\pm 1^\circ\text{C}$ ), showing that the methodology used to calculate  $T_{\text{mix}}$  is efficient.

As can be shown, for a CO<sub>2</sub> dispersion of  $\pm 27\%$ , a 10 % NO<sub>x</sub> emissions increase and a 51 % PM emissions increase are obtained, compared to the well mixed configuration.

## 5. Conclusion

In this study, the influence of cylinder-to-cylinder variations in EGR distribution on the resulting NO<sub>x</sub>-PM trade-off (while varying EGR rate) has been experimentally investigated on an automotive high-speed direct injection Diesel engine. Main conclusions are as follows:

- Unequal EGR distribution results in increased NO<sub>x</sub> and PM emissions compared to engine running with well mixed air and EGR gases.
- The increase in emissions is due to cylinder-to-cylinder variations in both gas composition and intake temperature.

From the above experiments, it is concluded that the suppression of unequal cylinder-to-cylinder EGR distribution results in a large reduction of NO<sub>x</sub> and PM emissions, especially when running with high EGR rates. An optimised air-EGR connection will be one of the ways to achieve future emissions standards.

## Appendix. Calculation of inlet temperature.

The mass flow conservation upstream and downstream of the air-EGR connection is given by:

$$\dot{m}_{\text{mix}} = \dot{m}_{\text{egr}} + \dot{m}_a \quad (\text{A1})$$

The thermodynamic first principle applied to the flow through air-EGR connection (supposed adiabatic) gives the enthalpy of air-EGR gases as follows:

$$h_{\text{mix}} = \frac{\dot{m}_a \cdot h_a + \dot{m}_{\text{egr}} \cdot h_{\text{egr}}}{\dot{m}_a + \dot{m}_{\text{egr}}} \quad (\text{A2})$$

Moreover, the CO<sub>2</sub> conservation is written as follows:

$$\frac{dn(\text{CO}_2)_{\text{egr}}}{dt} + \underbrace{\frac{dn(\text{CO}_2)_a}{dt}}_{=0} = \frac{dn(\text{CO}_2)_{\text{mix}}}{dt} \quad (\text{A3})$$

This can be written with CO<sub>2</sub> concentrations and volume flows:

$$D_{\text{egr}} \cdot [\text{CO}_2]_{\text{ex}} = (D_a + D_{\text{egr}}) \cdot [\text{CO}_2]_{\text{mix}} \quad (\text{A4})$$

$$\frac{\dot{m}_{\text{egr}}}{\rho_{\text{egr}}} \cdot [\text{CO}_2]_{\text{ex}} = \left( \frac{\dot{m}_a}{\rho_a} + \frac{\dot{m}_{\text{egr}}}{\rho_{\text{egr}}} \right) \cdot [\text{CO}_2]_{\text{mix}} \quad (\text{A5})$$

The EGR mass flow is finally given by:

$$\dot{m}_{\text{egr}} = \dot{m}_a \cdot \frac{\rho_{\text{egr}}}{\rho_a} \cdot \frac{[\text{CO}_2]_{\text{mix}}}{[\text{CO}_2]_{\text{ex}} - [\text{CO}_2]_{\text{mix}}} \quad (\text{A6})$$

EGR mass flow is thus deduced from the measured fresh air flow and CO<sub>2</sub> concentrations with equation (A6). Specific enthalpy of fresh air and EGR gases ( $h_a$  and  $h_{\text{egr}}$  respectively) are calculated according to gas compositions and temperatures. Equation (A2) gives specific enthalpy  $h_{\text{mix}}$  with 2.8 % CO<sub>2</sub> and 1.6 % CO<sub>2</sub>, and finally the corresponding temperature  $T_{\text{mix}}$ .

## References

- [1] J.B. Heywood, Internal combustion engine fundamentals, McGraw-Hill, New-York, 1988.
- [2] M. Zheng, G.T. Reader, J.G. Hawley, Diesel Engine Exhaust Gas Recirculation – A Review on Advanced and Novel Concepts. Energy Conversion and Management 45 (2004) 883-900.
- [3] A. Maiboom, X. Tauzia, J.-F. Hétet, Experimental study of various effects of exhaust gas recirculation (EGR) on combustion and emissions of an automotive direct injection Diesel engine, Energy 33 (2008) 22-34.
- [4] N. Ladommatos, S.M. Abdelhalim, H. Zhao, Z. Hu, The Dilution, Chemical, and Thermal Effects of Exhaust Gas Recirculation on Diesel Engine Emissions – Part 4: Effects of Carbon Dioxide and Water Vapor, SAE Paper 971660, 1997.
- [5] N. Ladommatos, S.M. Abdelhalim, H. Zhao, Z. Hu, Effects of EGR on Heat Release in Diesel Combustion, SAE paper 980184, 1998.

- [6] T. Jacobs, D. Assanis, Z. Filipi, The Impact of Exhaust Gas Recirculation on Performance and Emissions of a Heavy-Duty Diesel Engine, SAE paper 2003-01-1068, 2003.
- [7] R. Egnell, The Influence of EGR on Heat Release Rate and NO Formation in a DI Diesel Engine, SAE paper 2000-01-1807, 2000.
- [8] M.P.B. Musculus, On the Correlation Between NO<sub>x</sub> Emissions and the Diesel Premixed Burn, SAE paper 2004-01-1401, 2004.
- [9] B. Nitu, I. Singh, L. Zhong, K. Badreshany, N.A. Henein, W. Bryzik, Effect of EGR on Autoignition, Combustion, Regulated Emissions, and Aldehydes in DI Diesel Engines, SAE paper 2002-01-1153, 2002.
- [10] A.J. Torregrosa, P. Olmeda, J. Martin, B. Degraeuwe, Experiments on the influence of inlet charge and coolant temperature on performance and emissions of a DI Diesel engine, *Experimental Thermal and Fluid Sciences* 30 (2006) 633-641.
- [11] D.R. Tree, K.I. Svensson, Soot processes in compression ignition engines, *Progress in Energy and Combustion Science* 33 (2007) 272-309.
- [12] N. Ladommatos, S.M. Abdelhalim, H. Zhao, Control of Oxides of Nitrogen from Diesel Engines Using Diluents While Minimizing the Impact on Particulate Pollutants, *Applied Thermal Engineering* 18 (1998) 963-980.
- [13] D.A. Kouremenos, D.T. Hountalas, K.B. Binder, The Effect of EGR on the Performance and Pollutant Emissions of Heavy-Duty Diesel Engines Using Constant and Variable AFR, SAE paper 2001-01-0198, 2001.
- [14] D.T. Hountalas, Controlling Nitric Oxide and Soot in Heavy Duty Diesel Engines Using Internal Measures, FISITA World Automotive Congress, Barcelona, Spain, 2004.
- [15] D.T. Hountalas, J. Benajes, E.G. Pariotis, C.A. Gonzalez, Combination of High Injection Pressure and EGR to Control Nitric Oxide and Soot in DI Diesel Engines, THIESEL Conference on Thermo- and Fluid Dynamic Processes in Diesel Engines, Valencia, Spain, 2004.
- [16] R.M. Green, Measuring the Cylinder-to Cylinder EGR Distribution in the Intake of a Diesel Engine During Transient Operation, SAE paper 2000-01-2866, 2000.
- [17] R.M. Siewert, R.B. Krieger, M.S. Huebler, P.F. Baruah, B.M. Khalighi, M. Wesslau, Modifying an Intake Manifold to Improve Cylinder-to-Cylinder EGR Distribution in a DI Diesel Engine Using Combined CFD and Engine Experiments, SAE paper 2001-01-3685, 2001.
- [18] V.J. Page, C.P. Garner, G.K. Hargrave, H.K. Versteeg, Development of a Validated CFD Process for the Analysis of Inlet Manifold Flows with EGR, SAE paper 2002-01-0071, 2002.
- [19] W.P. Partridge, S.A. Lewis, M.J. Ruth, G.G. Muntean, R.C. Smith, J.H. Stang, Resolving EGR Distribution and Mixing, SAE paper 2002-01-2882, 2002.
- [20] J. William, A. Dupont, R. Bazile, M. Marchal, Study of Geometrical Parameter Influence on Air/EGR Mixing, JSAE paper 20030337, 2003.
- [21] A. Torres, S. Henriot, Modeling the Effects of EGR Inhomogeneities Induced by Intake Systems in a Four-Valve Engine, SAE paper 961959, 1996.

- [22] A. Taklanti, B. Delhay, Multi-Dimensional Modeling of the Aerodynamic and Combustion in Diesel Engines, *Oil & Gas Science and Technology* 54 (1999) 271-277.
- [23] K. Yoshizawa, K. Mori, Y. Matayoshi, S. Kimura, Development of an Exhaust Gas Recirculation Distribution Prediction Method Using Three-Dimensional Flow Analysis and Its Application, *Journal of Engineering for Gas Turbine and Power* 125 (2003) 1066-1074.
- [24] R.S.G. Baert, D.E. Beckman, A. Veen, Efficient EGR Technology for Future HD Diesel Engine Emissions Targets, SAE paper 1999-01-0837, 1999.
- [25] M. Rosslein, A. Williams, Quantifier l'incertitude dans les mesures analytiques, Guide Eurachem/CITAC 2nd edition, SLR Ellison.
- [26] A. Maiboom, X. Tauzia, J.-F. Hétet, M. Cormerais, M. Tounsi, T. Jaine, S. Blanchin, Various effects of EGR on combustion and emissions on an automotive DI Diesel engine: numerical and experimental study, JSAE paper 20077221, SAE paper 2007-01-1834, 2007.
- [27] K. Akihama, Y. Takatori, K. Inagaki, S. Sasaki, A.M. Dean, Mechanism of the Smokeless Rich Diesel Combustion by Reducing Temperature, SAE paper 2001-01-0655, 2001.
- [28] R.M. Wagner, J.B. Green, T.Q. Dam, K.D. Edwards, J.M. Storey, Simultaneous Low Engine-Out NO<sub>x</sub> and Particulate Matter with Highly Diluted Diesel Combustion, SAE paper 2003-01-0262, 2003.
- [29] C.S. Sluder, R.M. Wagner, S.A. Lewis, J.M. Storey, Exhaust Chemistry of Low-NO<sub>x</sub>, Low-PM Diesel Combustion, SAE paper 2004-01-0114, 2004.
- [30] N.H. Abu-Hamdeh, Effect of cooling the recirculated exhaust gases on diesel engine emissions, *Energy Conversion and Management* 44 (2003) 3113-3124.
- [31] D.T. Hountalas, G.C. Mavropoulos, K.B. Binder, Effect of exhaust gas recirculation (EGR) temperature for various EGR rates on heavy duty DI diesel engine performance and emissions. *Energy* 33 (2008) 272-283.

**Figure Captions**

Figure 1: Axial section (with respect to inlet duct) of air-EGR mixer

Figure 2: Configuration of engine inlet

Figure 3: NO<sub>x</sub>-PM trade-off while varying EGR rate with (w) and without (w/o) air-EGR mixer for operating points A and B (figure (a) and (b) respectively)

Figure 4: Mean gross ROHR (a), in-cylinder pressures (b), calculated core spray temperature (c) and flame temperature (d) while varying EGR rate with air-EGR mixer, operating point B.

Figure 5: CO<sub>2</sub> concentration at each inlet port with and without air-EGR mixer for various EGR rates, operating point A

Figure 6: NO<sub>x</sub>-PM trade-off while varying EGR under HTC mode, with  $T_{egr} = T_a$

Figure 7: NO<sub>x</sub>-PM trade-off while varying EGR under HTC mode, with  $T_{egr} > T_a$

Table 1. Specifications of test engine.

Type	turbocharged (VGT), intercooled
Compression ratio	18 : 1
Number of cylinders	4
Number of valves per cylinder	4
Combustion chamber type	re-entrant bowl-in-piston
Injection System	Common-rail piezoelectric 2 <sup>nd</sup> generation
Number of injection holes	7
Injection nozzle diameter (mm)	0.150
Maximum injection pressure (bar)	1600
Fuel	Diesel

Table 2. Operating conditions.

Point	Engine speed (rpm)	Pilot quantity (mg/stroke)	Principal quantity (mg/stroke)	BMEP (bar)	P <sub>rail</sub> (bar)
A	1450	1.5	17.7	5.5	700
B	1870	1.2	14.5	4.0	750



Table 3. Relative measurement error.

Instrument	Calibrated range	Accuracy	Relative error
Gas temperatures (k-type thermocouple)	0-1000 °C	$\pm 1^{\circ}\text{C}$	$\pm 0.75 \%$
Inlet gas pressure (2 bar piezoresistive relative pressure sensor HCS Sensor Technics)	0-2 bar	$\pm 5 \text{ mbar}$	$\pm 0.25 \%$
Air mass flow (hot wire air flow meter)	0-1000 mg/stroke	$\pm 5 \text{ mg/stroke}$	1 %
Fuel consumption (AVL PIERBURG PLU 401/121)	0.05-23 kg/h	$\pm 37 \text{ g/h}$	$\pm 0.16 \%$
NO <sub>x</sub> (ECO PHYSICS CLD 700EL)	0-1000 ppm	$\pm 5 \text{ ppm}$	1 %
Smoke (AVL 415S)	0-10 FSN	$\pm 0.1 \text{ FSN}$	2 %
Inlet and Exhaust CO <sub>2</sub> (SIEMENS ULTRAMAT 23)	0-20 %	$\pm 0.1 \%$	1 %

Table 4. Engine intake conditions and measured NOx and PM emissions.

Configuration	[CO <sub>2</sub> ] <sub>mix</sub> (rpm)	$\dot{m}_{egr}$ (mg/stroke)	T <sub>mix</sub> (°C)		NOx (g/h)	PM (g/h)
			calculated	measured		
Well mixed	2.20	71	45.3	44.8	<b>14.9</b>	<b>1.46</b>
Dispersed, cylinders 1,2	2.80	97	51.4	51.4	9.2	3.31
Dispersed, cylinders 3,4	1.60	48	39.4	39.4	23.6	1.09
Mean values:					<b>16.4</b>	<b>2.20</b>

Figure 1:

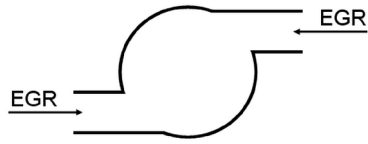


Figure 2:

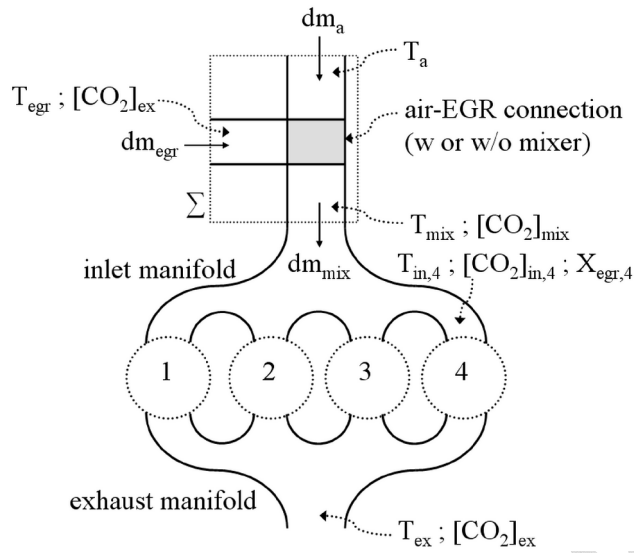


Figure 3:

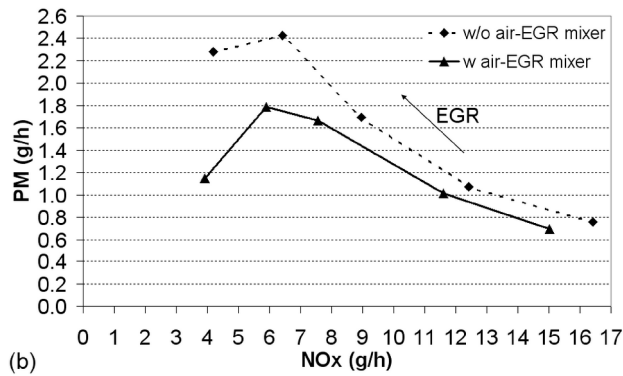
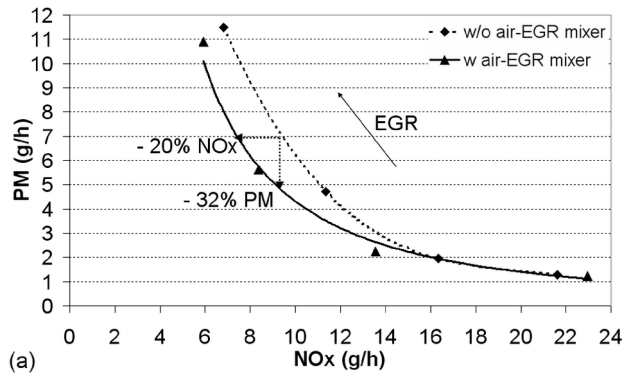
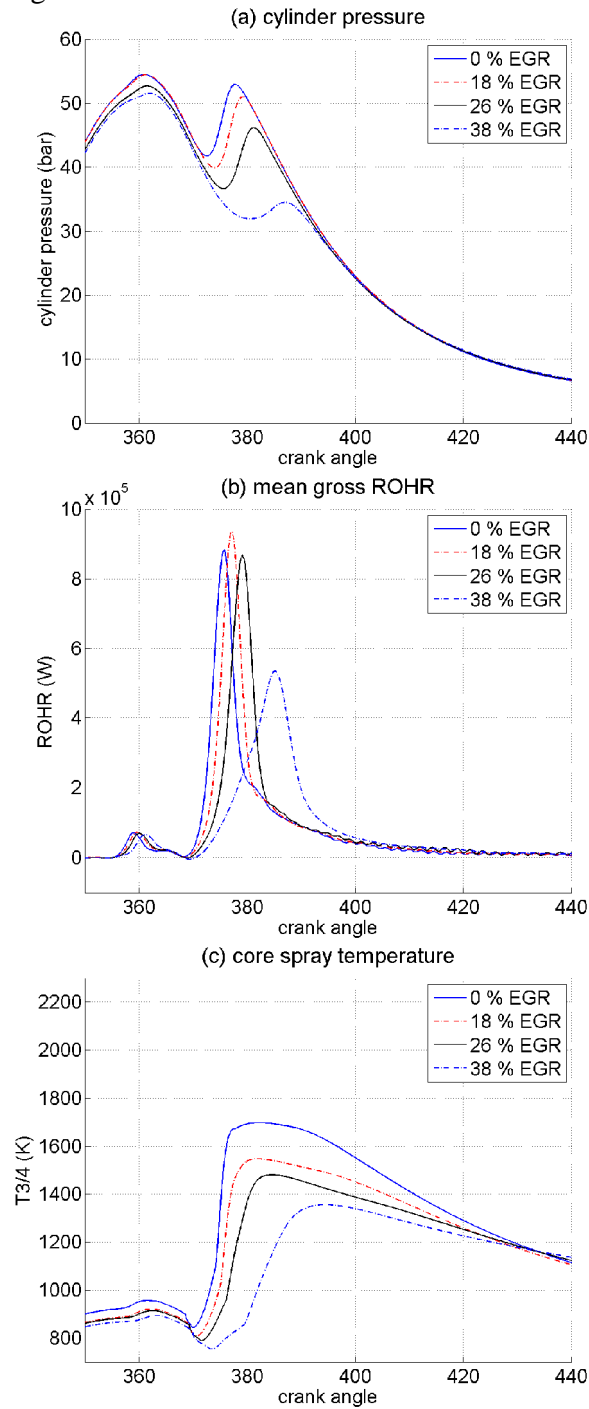


Figure 4:



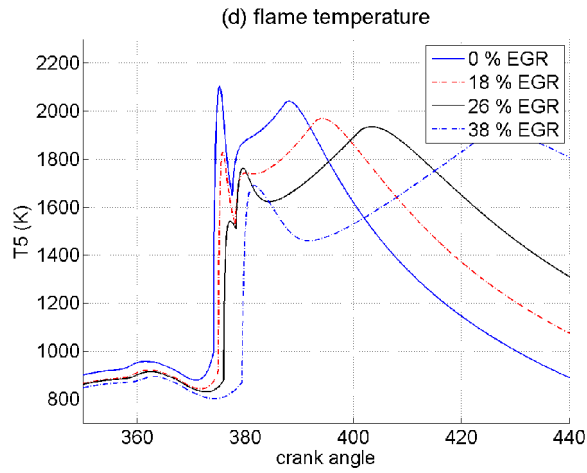


Figure 5:

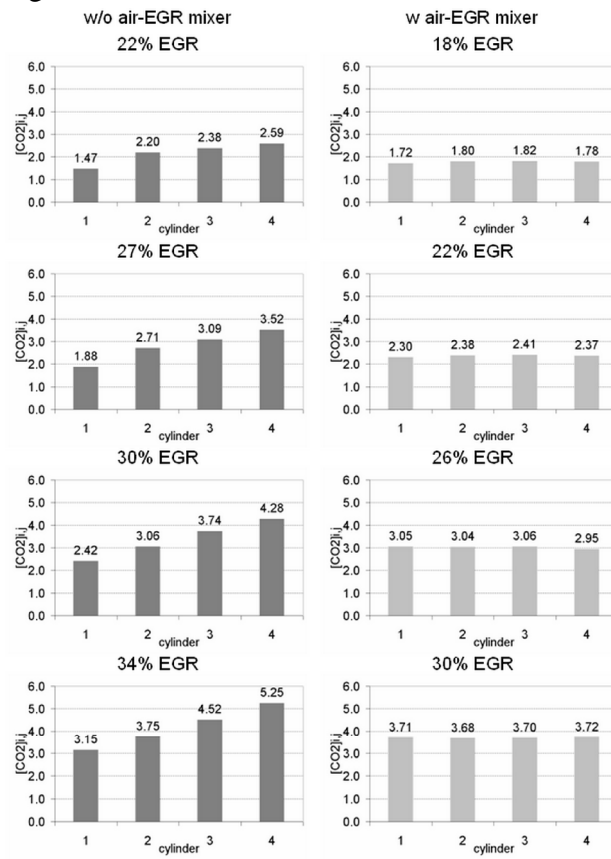
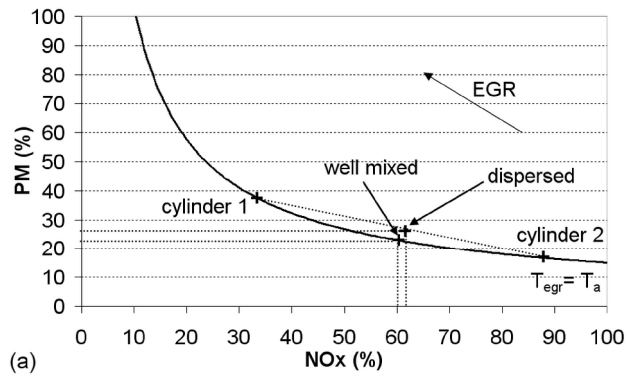
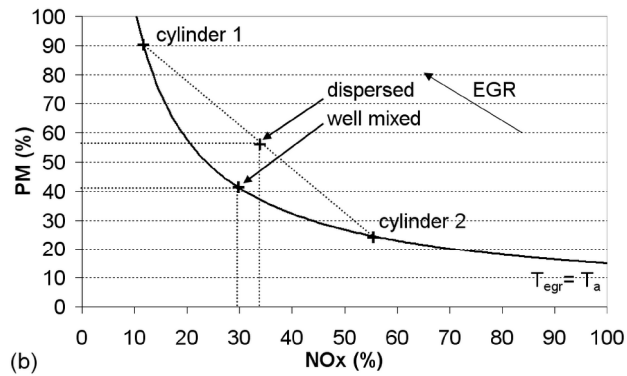


Figure 6:



(a)



(b)

Figure 7:

